

<Final Report: EEE4610-01>

Electromagnetic Interference Analysis and Measurement in High Power Charging Systems

Sungmin Jo

School of Electrical and Electronic Engineering

College of Engineering

Yonsei University

<Final Report: EEE4610-01>

Electromagnetic Interference Analysis and Measurement in High Power Charging Systems

Report Advisor: Eui-Bum Lee

December 2022

Sungmin Jo

School of Electrical and Electronic Engineering

College of Engineering

Yonsei University

감사의 글

4년 반이라는 시간이 빠르게 흐르고 어느새 대학교 4학년이 되면서 졸업 연구를 진행하게 되었습니다. 학부생들이 모두 필수로 진행해야 하는 전기전자종합설계 과목인 만큼 여러 연구실의 다양하고 흥미로운 주제들이 소개되었는데, 곧 취업을 앞두고 있는 저는 자동차 회사에 입사를 희망하기 때문에 육종관 교수님의 ACEM 연구실에서 진행되는 ‘고 전력 충전 시스템에서의 전자파 간섭 해석 및 측정’을 연구주제로 선택하게 되었습니다.

단순히 졸업요건을 충족시키기 위해 연구를 진행하는 것이 아니라, 이러한 경험이 훗날 저에게 큰 보탬이 되고 전기전자공학에 대한 시야를 넓힐 수 있는 계기가 되기를 간절히 소망하며, 이런 좋은 기회를 제공해주신 육종관 교수님, 이의범 연구원님, 그리고 연세대학교에게 감사의 말씀을 드립니다.

Contents

Figure index	iii
Table index	vi
Abstract	vii
1. Introduction	1
2. Background	3
2.1. EMC	3
2.2. Crosstalk	5
2.3. Power conversion system	7
2.3.1. Cable configuration	7
2.3.2. Converter	9
2.3.3. PFC	10
2.3.4. SMPS	11
2.4. DM noise and CM noise	12
3. Research method	14
3.1. Modeling the noise source applied to the dc line	15
3.1.1. Multi-conductor cable	15
3.1.1.1. General case of admittance and scattering matrix	16
3.1.1.2. Cable case of admittance and scattering matrix	18
3.1.2. Mathematical approach	20
3.1.2.1. Properties of admittance matrix	20
3.1.2.2. Performing the measurements at DC	21
3.1.3. Characteristics of actual cable model	24
3.2. Noise source modeling according to the topology of the power converter	25
3.2.1. DM noise source	28
3.2.2. CM noise source	30
4. Comparative verification of modeling-based analysis and simulation results	33
4.1. Based on noise source modeling applied to DC line	33
4.1.1. Verification of mathematical approach	33
4.1.2. Analyzing the characteristics of actual cable model	34
4.2. Based on noise source modeling according to the topology of the power converter	35
4.2.1. DM noise source	35
4.2.2. CM noise source	36
5. Review and discussion	37
6. Conclusion	39
Reference	41
국문요약	42

Figure index

Fig. 2.1. The block diagram of EMC	3
Fig. 2.2. Aspects of EMI	4
Fig. 2.3. Aspects of EMS	4
Fig. 2.4. Capacitive Coupling	5
Fig. 2.5. Inductive Coupling	5
Fig. 2.6. Duosida EVSE CCS Type 1 pin layout	7
Fig. 2.7. Bidirectional DC-to-DC converter circuits	9
Fig. 2.8. PFC block diagram	10
Fig. 2.9. Waveform of input voltage and current	11
Fig. 2.10. Noise current	13
Fig. 2.11. Radiation by noise	13
Fig. 3.1. Configuration of n-conductor cable	15
Fig. 3.2. Multi-port linear network	16
Fig. 3.3. Structure of the cable	18
Fig. 3.4. Equivalent circuit of the cable	19
Fig. 3.5. The number of groups of parameters	20
Fig. 3.6. DC equivalent circuit of the n-conductor cable	21
Fig. 3.7. Model of CCS Combo Type 1 cable	
Fig. 3.8. Lumped circuit of EMI noise coupling	25
Fig. 3.9. Simplified lumped circuit of EMI noise coupling	27
Fig. 3.10. DM model of EMI noise coupling	30
Fig. 3.11. DM modeling circuit using Simulink	30
Fig. 3.12. CM model of EMI noise coupling	30
Fig. 3.13. CM modeling circuit using Simulink	30
Fig. 4.1. Simulation setup	30
Fig. 4.2. C Matrix plot of the cable model	30
Fig. 4.3. Characteristic Impedance plot of the cable model	30
Fig. 4.4. R Matrix plot of the cable model	30
Fig. 4.5. Simulation result of voltage in DM modeling circuit	30
Fig. 4.6. Simulation result of current in CM modeling circuit	30
Fig. 4.7. Checking current with cursor	30
Fig. 4.8. Simulation result of voltage in CM modeling circuit	30
Fig. 4.9. Checking voltage with cursor	30

Table index

Table 2.1. CCS socket	8
Table 2.2. Linear control vs. Switching mode	12
Table 3.1. Impedances in DM and CM case	27

ABSTRACT

Electromagnetic Interference Analysis and Measurement in High Power Charging Systems

As interest in fast charging systems increases because of the development of electric vehicle related technologies and the need for fast charging systems that use high power to improve driver convenience increases, this study aims to compare and verify the modeling-based analysis and simulation results after modeling the noise source applied to the DC line and modeling the noise source according to the topology of the power converter. In the case of cable noise modeling, a DC equivalent circuit was first formed on the premise that the cable is a 3-conductor cable. At this time, since the circuit operates in the high-frequency region, the voltage and current values applied to the two ports on the same line are different, and EMI noise is generated between the lines. Therefore, modeling is carried out using the admittance matrix and the scattering matrix. The validity of the modeling was verified by substituting values for each device and parameter and conducting a simulation experiment. In the case of power converter noise modeling, since the lumped circuit of EMI noise coupling configuration changes as the conducted noise mode changes depending on the signal direction, it was divided into a DM model and a CM model. In DM noise modeling, the circuit is constructed using the shunt-insertion method, while the circuit is constructed using the series-insertion method in CM noise modeling. By substituting values for each device and parameter and conducting a simulation experiment, the validity of both modeling was verified.

Key words : EMI, multi-conductor cable, admittance matrix, scattering matrix, DM, CM

1. Introduction

Demand for electric vehicles has been increasing day by day since practical electric vehicles first appeared in 1890s. As environmental pollution is being deteriorated rapidly nowadays, the government and people began to seek eco-friendly measures in all fields. Among them, the automobile sector advocated carbon neutrality as a slogan and developed the technology and market for electric vehicles as the technology enhanced. Unlike general automobiles or petroleum-based transportations that use gasoline to operate with an internal combustion engine, electric vehicles do not emit smoke because they obtain driving power using electricity, and since it has been found that the increase in carbon dioxide caused by fossil fuels such as coal and oil promotes global warming, all countries around the world are spurring and staying focus on the development of electric vehicles to contribute to eco-friendliness. In case of the Korean government, as it promotes eco-friendly policies, various measures to encourage electric vehicles are being implemented such as offering subsidy for the purchase of an electric vehicle.

As the quantity of electric vehicles rapidly increased, the number of electric charging stations also increased. Although the development of batteries or battery charging technology continues steadily, it is on a troubling trend that cannot keep up with the current increase in the number of vehicles, and clearly there are technical limitations. A slow charger, which was mainly used when electric vehicles were commercialized in earnest and even still frequently used today, supplies alternating current to electric vehicles. Due to this feature, there are some advantages. Because it uses single-phase power, the structure design of the charger is simple and does not significantly affect the performance and lifespan of electric vehicle batteries. However, slow charging takes a very long time, with an average charging time of 7 to 12 hours, which can cause several problems such as insufficient space at charging stations, necessity to prepare alternative measures in case of charger failure, and establishment of electric vehicle charging infrastructure.

In order to compensate for the problem of slow charging, boost charging technology is being developed. Fast charging takes about 30 minutes to an hour on average for an electric vehicle to be fully charged, and it can be seen that the charging time is significantly reduced compared to slow charging. Also, unlike slow chargers that use single-phase power, boost chargers require three-phase power structure, and since they supply direct current to electric vehicles, an AC-DC converter is needed inside the charger.

However, boost charging also has several problems. First of all, the output is very large because it uses high power, so the construction is difficult, and its installation cost is also very high. In addition, more heat is generated because high power is used, and in proportion to this, the wire becomes thicker, which means that it becomes less flexible and much heavier. Contrary to the advantages of slow charging, continuous use of fast charging may cause various problems such as deterioration of battery performance and shortening the lifespan. In terms of self-consumption, it is not higher than gasoline of course, but the power charging fee is about 200 won(per kW) more expensive compared to slow charging. Although there are many disadvantages of high-power charging system, the part to be dealt with in this paper is electromagnetic interference.

Cables used in fast chargers largely include a power line using a high frequency signal and a communication line using a low frequency signal. Due to these characteristics, electromagnetic waves or noises are generated by the power line through which a high-power current flow, which affects the communication line. As a result, interference in the received signal causes information damage or breaks the boost charging cable frequently. In response to this, various methods have been proposed to solve problems from the past to the present, and research is being actively conducted as innovative technologies are developed. Therefore, in order to solve the problems caused by electromagnetic interference, I intend to analyze and measure electromagnetic waves through the noise source modeling technique, thanks to the research that has been conducted so far and the interest that has been poured in.

2. Background

Before the research, since high power charging systems deal with numerous electrical features, we need to clearly figure out electromagnetic wave related concepts and terms in order to understand them. In addition, to clearly get the idea of what principles electromagnetic waves are generated and why the interference occurs, the configuration and design of boost chargers and cables must be carefully explored.

2.1 EMC

EMC is an abbreviation of Electromagnetic Compatibility, which is also a comprehensive term containing two opposite concepts which are EMI and EMS, as illustrated in Fig. 1.1. It generally refers to the ability to ensure that unnecessary electromagnetic waves from electrical or electronic devices do not affect any other equipment or systems, and conversely, operate properly even if they receive electromagnetic interference from the other equipment or systems.

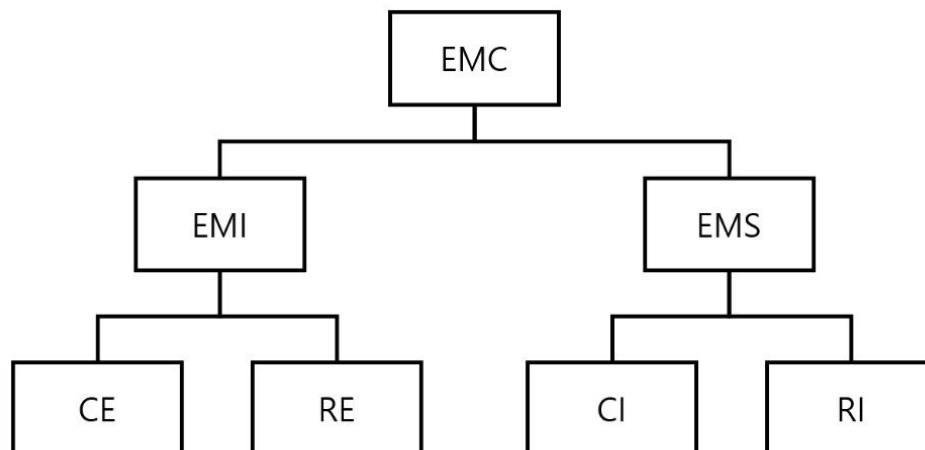


Fig. 1.1 The block diagram of EMC

EMI stands for Electromagnetic Interference, which means that a device that emits unnecessary electromagnetic waves to the outside under Ampere's law and interferes with other devices or control circuits in the form of CE(Conducted Emission) and RE(Radiated Emission). It could be radiated into space or conducted through power lines to cause electromagnetic disturbances in their own devices or other devices.

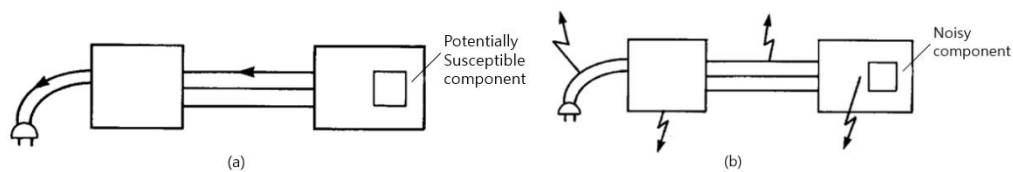


Fig. 2.2 Aspects of EMI: (a) Conducted emission; (b) Radiated emission

EMS stands for Electromagnetic Susceptibility, which is a opposite concept of EMI, meaning the ability of a device or system to operate without adverse effects in performance even in the presence of electromagnetic interference from other devices in the form of CI(Conducted Immunity) and RI(Radiated Immunity).

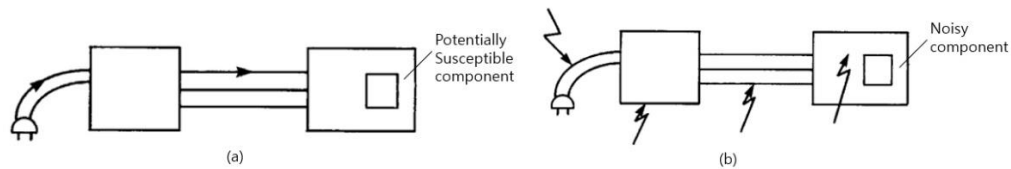


Fig. 2.3 Aspects of EMS: (a) Conducted immunity; (b) Radiated immunity

2.2 Crosstalk

Crosstalk refers to the unwanted propagation of signals and noise between coupled lines. In case of two wires being separate, it is unlikely that electrical signals and noise be conducted. However, if they are in parallel, the noise is conducted because of the stray capacitance and mutual inductance that exist in the middle of two wires. Thus, crosstalk can be referred to as conducted noise. To be specific, coupling between lines includes capacitive coupling by stray capacitance, also known as parasitic capacitance, and inductive coupling by mutual inductance, in which both of them cause noise. Fig. 2.4 and Fig. 2.5 shows the illustrations and simplified equivalent circuits for each case.

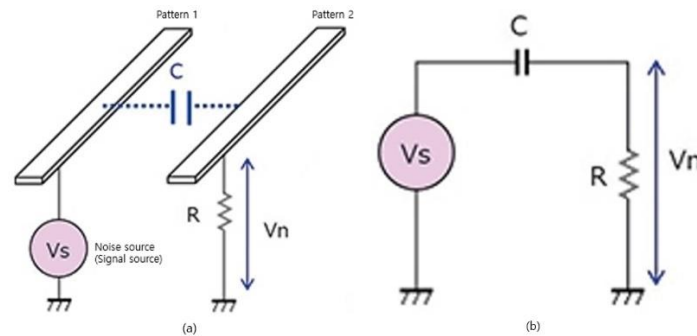


Fig. 2.4 Capacitive Coupling: (a) Illustration; (b) Equivalent circuit

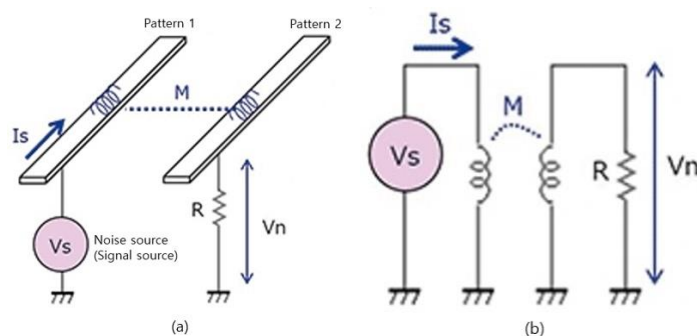


Fig. 2.5 Inductive Coupling: (a) Illustration; (b) Equivalent circuit

In case of a cable, crosstalk normally represents electromagnetic interference between an unshielded twisted pair and a twisted pair, which are located in parallel, and there are basically Near-end crosstalk and Far-end crosstalk.

NEXT means a phenomenon in which crosstalk is generated from the inducing line of the transmitting side to the guided line of the transmitting side, and it's also the main environmental noise occurring in the general subscriber line, which implies that the source of the crosstalk and the listener are at the same end. Moreover, NEXT is inversely proportional to the frequency and the length of the line or cable, so the larger the number, the less the unintentional induced signal or interference signal is generated. It is most likely to happen when several pairs of communication lines are bundled up and installed while sending an electric signal in a two-wire type using two parallel wires or a single-wire type in which one side is grounded. Even if the signal lines through which a weak electrical signal flows are partially adjacent to each other within a short distance, the effect on each other is relatively small, but if they are adjacent to each other over a long distance in a parallel state, electromagnetic interference will overlap and have a huge impact on each other. Therefore, twisted or shielded cables are utilized as a solution to this problem.

FEXT is a phenomenon in which the transmitted signal affects the other guided line on the receiving side from its own receiving side guided line, and it also calculates the interference between the two pairs of a cable measured at the far end, regarding the interfering transmitter. That is, the source of the crosstalk and the listener are at different ends. In general, the near-end crosstalk has more influence than the far-end crosstalk.

2.3 Power conversion system

Electric vehicles cannot directly use an alternating current input as an output in the form of AC. Since it has to be converted to direct current, a power conversion system is essentially required. The system largely consists of AC/DC and DC/DC converter, Power Factor Correction, and Switching Mode Power Supply. But firstly, we'll look into a cable configuration and then figure out the concepts of the system components.

2.3.1 Cable configuration

Combined Charging System that uses Combo 1 and 2 connectors providing power 350kW maximum is a basic system for charging EV. These connectors are attached to the existing AC vehicle connectors, allowing high power DC boost charging by putting two additional DC contacts. EVSE, which stands for Electric Vehicle Supply Equipment, supplies electricity to an electric vehicle, containing components that rectify the AC power to DC. The concepts are well illustrated in Fig. 2.6.

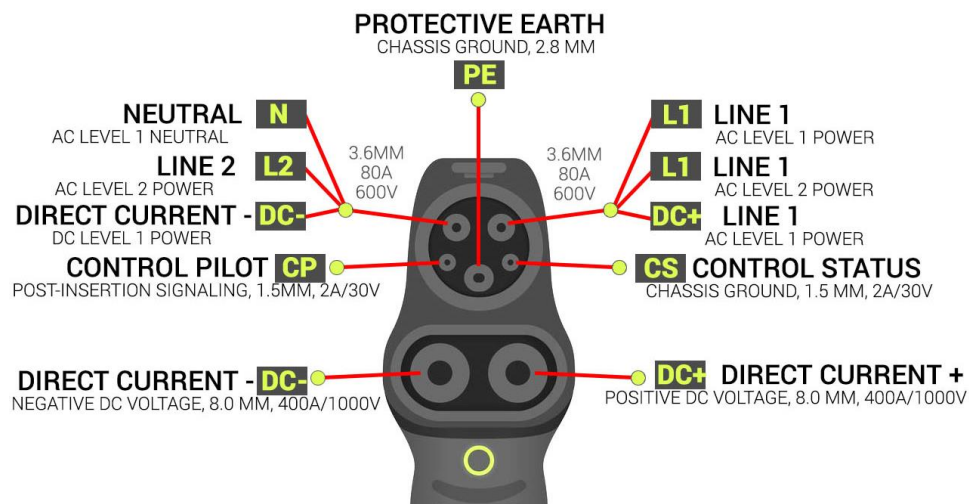


Fig. 2.6 Duosida EVSE CCS Type 1 pin layout

The vehicle coupler is mainly consisting of the vehicle connector and the vehicle inlet. Referring to Table 2.1, the CCS couplers are based on the North American and European standard, which are Type1 and Type 2 respectively. Developing a vehicle inlet to make the AC connectors that previously existed, and DC contacts added later valid at the same time was the biggest problem that the CCS had ever faced, but eventually both of the couplers succeeded being compatible by attaching the two DC contacts below the AC connectors and communication contacts.




Type	Boost charging port		
	DC Combo Type 1	DC Combo Type 2	CHAdeMO
Connector			
	AC 220V AC 220V GND CP PD DC(+) DC(-)	AC 220V AC 220V AC 220V Neutral GND CP PD DC(+) DC(-)	GND Start/Stop 1 Start/Stop 2 DC(+) DC(-) ENABLE CAN(L) CAN(H) PD
Country of use	US, South Korea	Europe	US, South Korea, Europe, Japan
Charging condition	120A(50kW), 172A(100kW)		
Charging capacity	50kW/100kW		
Communication	PLC (Power Line Communication)		CAN

Table 2.1 CCS socket

2.3.2 Converter

A converter is a device that can convert electrical energy, and it can change the alternating current to direct current and vice versa. The converter is used in many different ways, and it ranges from a very simple system such as a transformer to a complex system like a resonant converter. In general, the main purpose of the converter is controlling and processing the flow of electrical energy by supplying the most suitable current and voltage for intended uses or user loads. There are several types of conversion, but we would like to focus on only two types, which are AC/DC converter and DC/DC converter.

An AC/DC converter is the most and widely used because almost all of the home appliances use DC voltage, so it is necessary to convert AC transmitted from the power plant to DC for practical use. Rectifier or motor-generator is a typical example of the converter.

A DC/DC converter is a device that converts a voltage level of a direct current source, and the range of power levels is very wide, from batteries(low) to power transmission(high). In case of buck converter, as illustrated in Fig. 2.7 (a), is a power converter that steps down the voltage. In contrast, boost converter steps up the voltage while stepping down the current, which is also illustrated in Fig. 2.7 (b). We will be dealing with these concepts further in 2.3.4 SMPS(Switching Mode Power Supply).

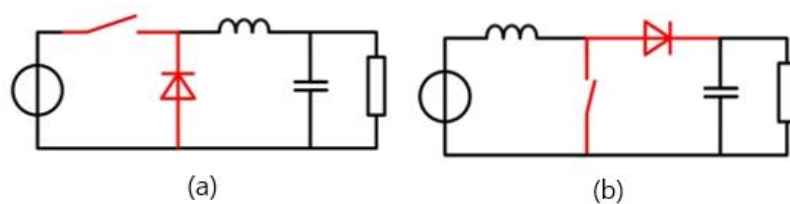


Fig. 2.7 Bidirectional DC-to-DC converter circuits: (a) Buck (b) Boost

2.3.3 PFC

PFC(Power Factor Correction) consists of a diode rectifier that converts AC input to DC and a boost converter which converts the magnitude of the PFC output voltage, and a brief configuration of PFC is shown in Fig. 2.8. The purpose of using the PFC is to improve the power factor by reducing the phase gap between voltage and current produced in the middle of converting the form of power.

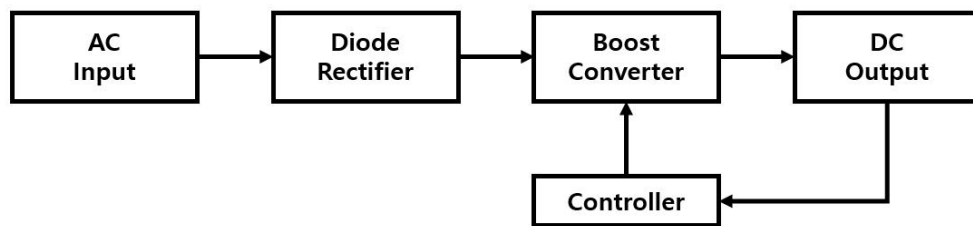


Fig. 2.8 PFC block diagram

When AC is converted to DC using only a diode rectifier without utilizing PFC, a phase difference between the voltage and the current occurs as shown in Fig. 2.9 (a), leading a decrease in power factor which reduces efficiency, increasing THD(Total Harmonic Distortion), and causing a problem of cost increase due to the growth of the rated current of the device applied in the circuit.

To solve this problem, we use PFC in order to make the phase gap between the current and the AC input voltage minimized as shown in Fig. 2.9 (b), through the control of the boost converter following the diode rectifier. As a result, the apparent power approaches the active power, which leads to an increase in efficiency. At the same time, we can look forward to improving the system stability by suppressing the generation of harmonic components of the current, thereby lowering the THD. The DC output voltage of the PFC is used as the input of the DC/DC converter as well as an input of SMPS.

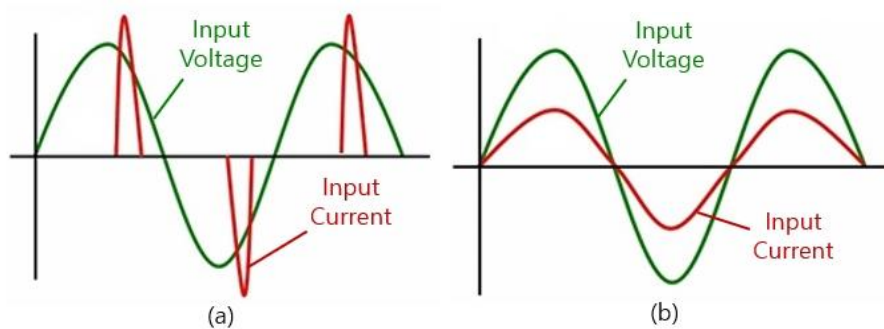


Fig. 2.9 Waveform of input voltage and current: (a) PFC not applied; (b) PFC applied

2.3.4 SMPS

A Switching Mode Power Supply contains a switching regulator that converts power efficiently. SMPS receives power from a power source just like the other power supplies, changes current or voltage characteristics, and then transmits the power to an electronic device such as a refrigerator. Unlike a control power supply which is linear, the pass transistor of an SMPS is constantly on and off, but only for a very short time to minimize power loss, oscillating between a low point and a high point of loss.

The voltage regulator operates by the on-off time ratio. On the other hand, a linear control power supply operates by rectifying the output voltage by the power continuously lost in the pass transistor. High power conversion efficiency is one of the advantages of SMPS shown in Table 2.2, and it can also be made considerably smaller and lighter, since they can further decrease the size and weight of the transformer compared to linear control power supplies. Switching regulators can be used instead of linear regulators when their efficiency is high enough, and they must be small in size or light in weight. It is also more complicated because noise is generated during switching conversion of current, and power efficiency can be lowered if the design is not taken care of.

Type	Linear control power supply	Switching mode power supply
Efficiency	Low(20~50%)	High(65~90%)
Stability	High	Normal
Noise & Ripple	Small(~10mv)	Large(10~200mV)
Response rate	Fast	Normal
Input voltage	Small range	Large range
Circuit	Simple	Complex
Dimensions	Large	Small
Weight	Heavy	Light

Table 2.2 Linear control vs. Switching mode

2.4 DM noise and CM noise

We previously figured out that EMI is classified into conducted noise and radiated noise. Among them, conducted noise can be divided into DM(Differential mode) and CM(Common mode) by the method of conduction. We will briefly go through the details of the DM noise and CM noise for now and discuss further in 3.2(Noise source modeling according to the topology of the power converter)

The DM noise occurs between the power lines as the noise source comes in series with respect to them since the noise current flows in the same direction as the power line, and its directions of output and input are opposite as in Fig. 2.10 (a).

The CM noise occurs in the method of the noise current leaked through parasitic capacitors returning to the power line through the ground. As in Fig. 2.10 (b), the direction of the noise current flowing from the positive side and the negative side of the power supply is the same, and no noise voltage is generated between the power lines.

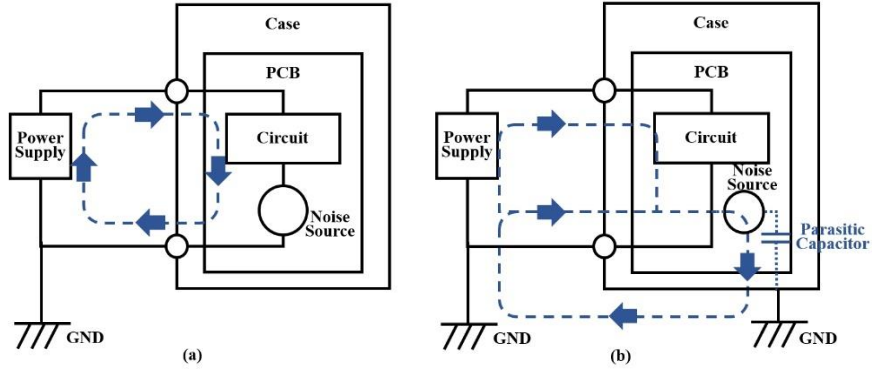


Fig. 2.10 Noise current: (a) Differential mode; (b) Common mode

The electric field strength of radiation due to DM noise (E_d) can be expressed by the equation $E_d \propto \frac{I_d \times f^2 \times S}{r}$, and I_d , f , S and r represent noise current, noise frequency, loop area, and distance to the viewpoint respectively. On the other hand, the electric field strength of radiation due to CM noise (E_c) is expressed by the equation $E_c \propto \frac{I_c \times f \times L}{r}$, and I_c , L represent noise current and cable length respectively. The loop area S is an important factor determining the field strength in DM, and the cable length is a crucial factor in case of CM.

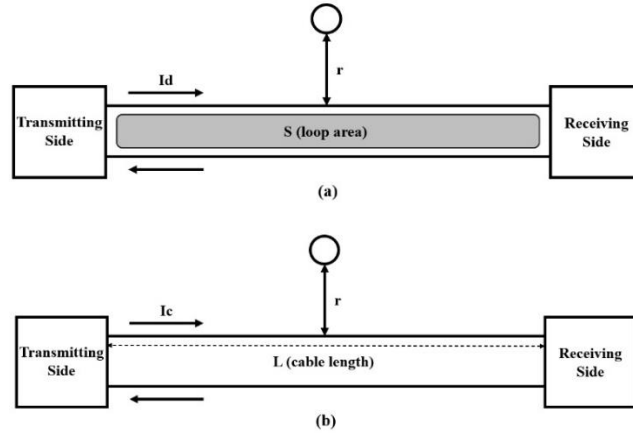


Fig. 2.11 Radiation by noise: (a) Differential mode; (b) Common mode

3. Research method

As we start to go through the research method, we will focus on two main research goals. The first goal is modeling the noise source applied to the DC line, and the second goal is modeling the noise source according to the topology of the power converter.

In the first study, which is the "modeling the noise source applied to the DC line", we must first consider the multi-conductor cable modeling in the general case, which is the basis and basic of this experiment, and then we have to narrow the scope into a special case which is modeling the 3-conductor cable, used in a real-life fast charging cable for electric vehicles. After that, we would like to take the next step by introducing mathematical methods such as rational function approximation, using the values derived from the previous step, and then a simulation project will proceed referred to the function. Finally, there will be a brief introduction about how the experiment using the actual cables is structured and how its procedure is done in the multi-conductor cable case.

In the second study, which is the "noise source modeling according to the topology of the power converter", theory and general contents are introduced at the beginning. The next step will be an explanation of the experimental method for the DM noise source, and then the experimental method for the CM noise source will be introduced. In the final stage, as in previous studies, there will be a brief introduction about how the simulation experiment is structured and how the procedure is carried out in case of the power converter.

The detailed analysis and comparison between the mathematical approach and simulation results of each experiment is presented in 4. Comparative verification of modeling-based analysis and simulation results.

3.1 Modeling the noise source applied to the dc line

When we look inside the cross section of the fast-charging cable for electric vehicle, there are several bundles of thin wires, and it can be considered that they are having the same effect as multi-conductor with respect to EMI. Therefore, we will assume the fast-charging cable as the multi-conductor cable and move on.

The multi-conductor cable is also referred to n-conductor cable, which means that the cable having n conductors that are insulated from one another, and the letter "n" signifies the number of insulated conductors in the cable. Using this method and creating an appropriate function to predict EMI is an essential process in the noise source modeling.

3.1.1 Multi-conductor cable

When we see the cable as a multi-port linear network, and assuming that there are n conductors in one cable, an electrical network which has $2n$ ports and has a difference of n between the ends of each conductor is created, as illustrated in Fig. 3.1. The outermost part of the cable that surrounds n conductors refers to a shield and is usually called a reference conductor. If there is no shield, then any one of the conductors inside the cable can be regarded as the reference conductor instead.

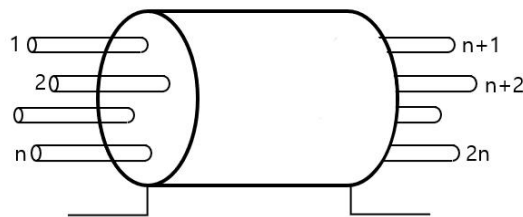


Fig. 3.1 Configuration of n-conductor cable

3.1.1.1 General case of admittance and scattering matrix

Let the current which is flowing through each signal conductor be i , and let the voltage across each end of the signal conductor, i.e., the potential difference between the signal conductor and the reference conductor be v . Then the multi-port linear network can be expressed as $i = Yv$, where Y represents the admittance matrix, and it can also be expressed as the following determinant:

$$\begin{bmatrix} i_1 \\ \vdots \\ i_{2n} \end{bmatrix} = \begin{bmatrix} y_{1,1} & \cdots & y_{1,2n} \\ \vdots & \ddots & \vdots \\ y_{2n,1} & \cdots & y_{2n,2n} \end{bmatrix} \begin{bmatrix} v_1 \\ \vdots \\ v_{2n} \end{bmatrix} \quad \dots \textcircled{a}$$

Each element in the admittance matrix Y can be identified through the equation

$$y_{i,j} = \frac{i_i}{v_j} \bigg|_{v_k=0, k \neq j} \quad \text{by means of making all ports except } i \text{ and } v \text{ related to the desired}$$

parameter a short circuit. Fig. 3.2 (a) shows the above contents implicitly.

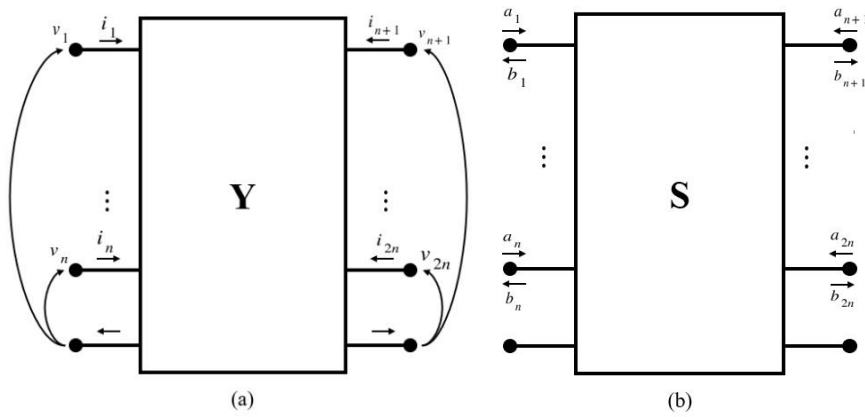


Fig. 3.2 Multi-port linear network: (a) Admittance matrix; (b) Scattering matrix

When looking at the multi-conductor cable from the multi-port linear network point of view, not only that the current flows in one direction in one port as shown in Fig. 3.2 (a) but also the fact that two types of waves flow in the opposite direction to each other in one port as shown in Fig. 3.2 (b), which are incident power wave and reflected power wave, must be considered too.

When expressing mathematically in the latter case, we use the equation $b = Sa$, which a means an incident power wave, b means a reflected power wave, and S represents the scattering matrix. Thus, the following determinant is used:

$$\begin{bmatrix} b_1 \\ \vdots \\ b_{2n} \end{bmatrix} = \begin{bmatrix} s_{1,1} & \cdots & s_{1,2n} \\ \vdots & \ddots & \vdots \\ s_{2n,1} & \cdots & s_{2n,2n} \end{bmatrix} \begin{bmatrix} a_1 \\ \vdots \\ a_{2n} \end{bmatrix} \dots \textcircled{b}$$

We can get the values of a and b by the equations $a_i = \frac{v_i + Z_{0i}i_i}{2\sqrt{Z_{0i}}}$ and

$b_i = \frac{v_i - Z_{0i}i_i}{2\sqrt{Z_{0i}}}$, which Z_0 represents the reference impedance for the ports. Each element in

the scattering matrix S can be obtained through the equation $s_{i,j} = \left. \frac{b_i}{a_j} \right|_{a_k=0, k \neq j}$ by

connecting all ports not related to the desired parameter with the reference load Z_0 .

3.1.1.2 Cable case of admittance and scattering matrix

Previously, we figured out the general case which was the n-conductor cable, and we are going to apply this concept to the actual cable which is basically 3-conductor cable.

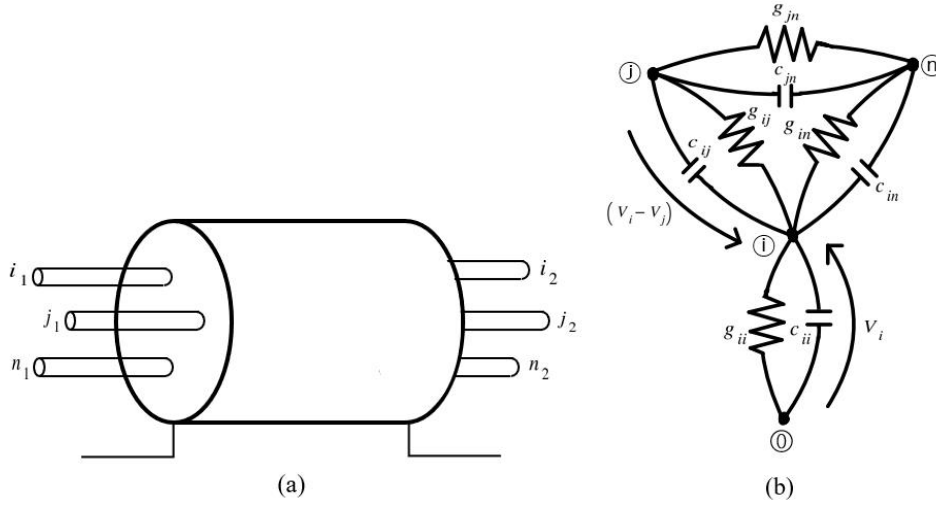


Fig. 3.3 Structure of the cable: (a) Configuration; (b) Circuit

When we use the equation (a) in 3.1.1.1, the multi-port linear network related to admittance matrix can be represented by the following determinant:

$$\begin{bmatrix} i_{i_1} \\ i_{j_1} \\ i_{n_1} \\ i_{i_2} \\ i_{j_2} \\ i_{n_2} \end{bmatrix} = \begin{bmatrix} y_{i_1, i_1} & y_{i_1, j_1} & y_{i_1, n_1} & y_{i_1, i_2} & y_{i_1, j_2} & y_{i_1, n_2} \\ y_{j_1, i_1} & y_{j_1, j_1} & y_{j_1, n_1} & & & \\ y_{n_1, i_1} & y_{n_1, j_1} & y_{n_1, n_1} & & & \\ y_{i_2, i_1} & & & & & \\ y_{j_2, i_1} & \vdots & \vdots & \vdots & \ddots & y_{j_2, n_2} \\ y_{n_2, i_1} & & & y_{n_2, j_2} & y_{n_2, n_2} & \end{bmatrix} \begin{bmatrix} v_{i_1} \\ v_{j_1} \\ v_{n_1} \\ v_{i_2} \\ v_{j_2} \\ v_{n_2} \end{bmatrix} \dots \textcircled{c}$$

The actual cable structure is expressed as an equivalent circuit as shown in Fig. 3.4.

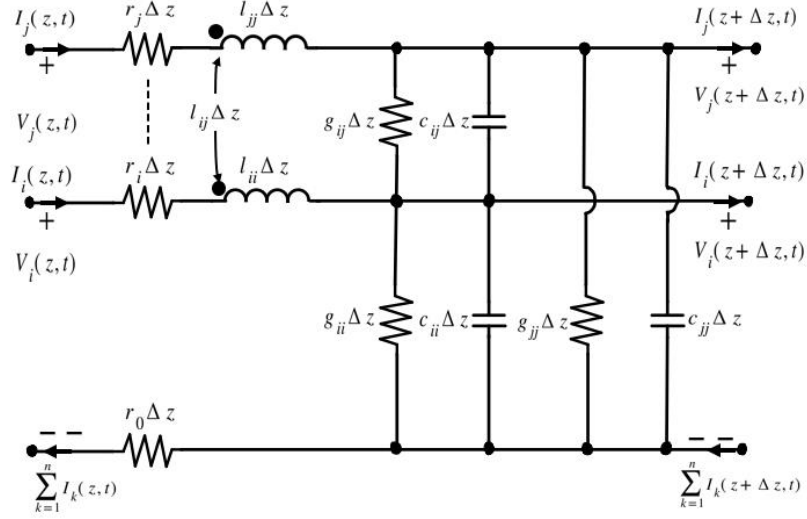


Fig. 3.4 Equivalent circuit of the cable

Using the equation ⑥ in 3.1.1.1 similar to the admittance matrix case, the multi-port linear network related to scattering matrix can be defined as the following determinant:

$$\begin{bmatrix} b_{i_1} \\ b_{j_1} \\ b_{n_1} \\ b_{i_2} \\ b_{j_2} \\ b_{n_2} \end{bmatrix} = \begin{bmatrix} s_{i_1,i_1} & s_{i_1,j_1} & s_{i_1,n_1} & s_{i_1,i_2} & s_{i_1,j_2} & s_{i_1,n_2} \\ s_{j_1,i_1} & s_{j_1,j_1} & s_{j_1,n_1} & & & \\ s_{n_1,i_1} & s_{n_1,j_1} & s_{n_1,n_1} & & & \\ s_{i_2,i_1} & & & & & \\ s_{j_2,i_1} & \vdots & \vdots & \vdots & \ddots & s_{j_2,n_2} \\ s_{n_2,i_1} & & & s_{n_2,j_2} & s_{n_2,n_2} & \end{bmatrix} \begin{bmatrix} a_{i_1} \\ a_{j_1} \\ a_{n_1} \\ a_{i_2} \\ a_{j_2} \\ a_{n_2} \end{bmatrix} \dots \textcircled{d}$$

We can get the values of each parameter by utilizing simple algebraic transformations

$$S = (1 + Z_0 Y)^{-1} (1 - Z_0 Y) \dots \textcircled{e} \quad \text{and} \quad Y = \frac{1}{Z_0} (1 + S)^{-1} (1 - S) \dots \textcircled{f}$$

3.1.2 Mathematical approach

First of all, we will go through details of basic properties of admittance matrix, and then figure out how the measurements of y-parameters can be performed by a method of direct current modeling. Next, we're going to setup the equations and matrices specifically.

3.1.2.1 Properties of admittance matrix

We mostly use symmetries to reduce the complexity of modeling. There are two types of symmetries, the first is about the midpoint of the conductor's length and the second is about the rotation with regard to the center of the circle when looking at the cross-section of the conductor. Putting all this together, in the case of n-signal conductor cable, the parameters appear as $2(\lfloor n/2 \rfloor + 1)$ distinct groups. For example, if 4 signal conductors exist and have symmetry properties as shown in Fig. 3.5 (a), the parameters are represented in 6 groups by the equation $2(\lfloor 4/2 \rfloor + 1)$, and if there are 3 signal conductors like an actual cable as shown in Fig. 3.5 (b) having the properties of symmetry, the parameter is expressed in 4 groups by the equation $2(\lfloor 3/2 \rfloor + 1)$.

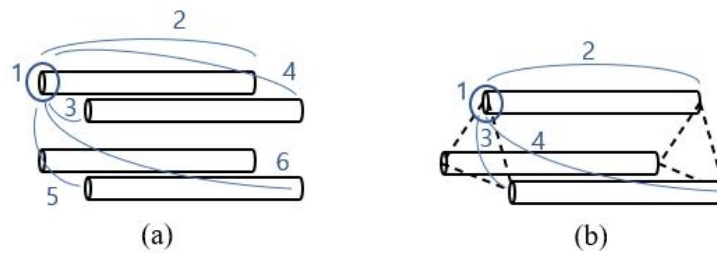


Fig. 3.5 The number of groups of parameters: (a) 4 signal conductors; (b) 3 signal conductors

In a high frequency condition, it is much more convenient to get the values of s-parameters than y-parameters, and a typical 2-port VNA(Vector Network Analyzer) is used in the procedure. After we knew the scattering matrix, we can also get admittance matrix easily by using the equation ⑥ in 3.1.1.2.

3.1.2.2 Performing the measurements at DC

In case of the DC measurement, we utilize a simple multimeter, measuring the resistances between the opposite ends within a conductor, and between the signal conductor and the reference conductor. This process is possible because there aren't any inductive or capacitive coupling between conductors since it's in a condition of DC.

DC equivalent circuit of the n-conductor cable is described in Fig 3.6, where R is the resistance of the signal conductor, R_g is the leakage resistance which should be large enough to increase the stability margin of the model and avoid any type of convergence problems, and R_{sh} is the resistance of the reference conductor.

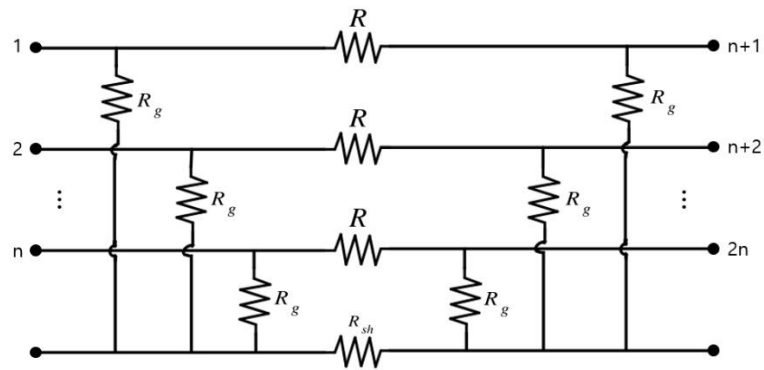


Fig. 3.6 DC equivalent circuit of the n-conductor cable

We can also define the admittance matrix of the equivalent circuit by the equation

$$Y_{dc} = \begin{bmatrix} Y_s & Y_m \\ Y_m & Y_s \end{bmatrix} \dots \textcircled{a}, \text{ where } Y_s = \begin{bmatrix} y_s & y_{m1} & \cdots \\ y_{m1} & y_s & \cdots & \vdots \\ \vdots & \vdots & \ddots & y_{m1} \\ \cdots & y_{m1} & y_s \end{bmatrix}_{n \times n} \dots \textcircled{b}$$

$$Y_m = \begin{bmatrix} y_m & -y_{m1} & \cdots \\ -y_{m1} & y_m & \cdots & \vdots \\ \vdots & \vdots & \ddots & -y_{m1} \\ \cdots & -y_{m1} & y_m \end{bmatrix}_{n \times n} \dots \textcircled{c}$$

and

$$y_s = \frac{1}{R_g} + \frac{1}{R + \frac{1}{(n-1)/R + 1/R_{sh}}} \dots \textcircled{d}$$

$$y_m = - \frac{1}{R + \frac{1}{(n-1)/R + 1/R_{sh}}} \dots \textcircled{e}$$

$$y_{m1} = \frac{1}{n-1 + R/R_{sh}} \frac{1}{R + \frac{1}{(n-1)/R + 1/R_{sh}}} \dots \textcircled{f}$$

3.1.3 Characteristics of actual cable model

Since we have gone through the modeling of the 3-conductor cable in a mathematical way previously, we would like to know the characteristics of the actual cable, which is the CCS Combo Type 1 cable, introduced in 2.3.1. We will model the cable structure of CCS Combo Type 1 by use of Ansys Electronics program as illustrated in Fig. 3.7, and then figure out the features of the model within the frequency range of 150kHz~30MHz, because the whole cable modeling process is done and also valid in the high frequency region.

Looking at the cable model, it has a configuration of PE, DC plus, DC minus, CP, PP, dummy2 and dummy3. We can find out that there are some differences between the lines, such as the diameters and the distances between the lines. Using the simulation in Ansys Electronics program, we're going to plot impedances with regard to the frequency and analyze the results of each plot, and then associate it with the works we've done before.

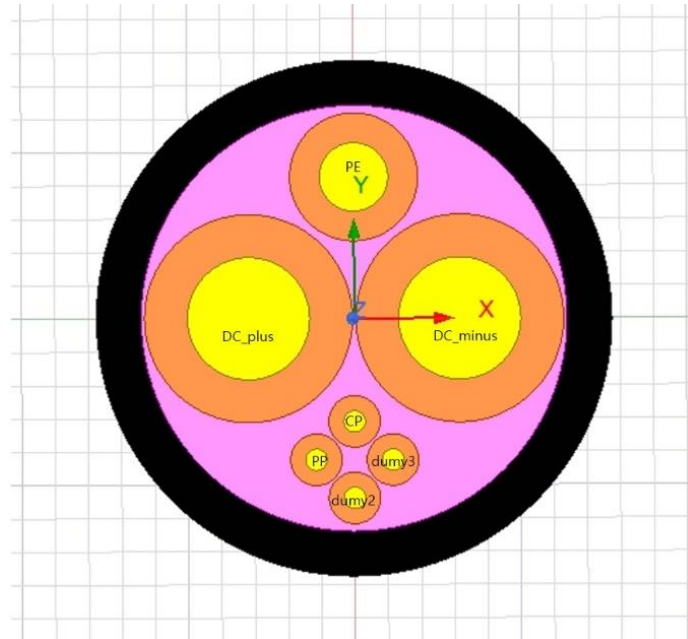


Fig. 3.7 Model of CCS Combo Type 1 cable

3.2 Noise source modeling according to the topology of the power converter

The power converter generates EMI by fast switching actions in the high frequency region. Among the two types of EMI, which are conducted emission and radiated emission, we will look into the conducted EMI noise measurement.

As shown in Fig. 3.8, the lumped circuit of EMI noise coupling is composed of LISN(Line Impedance Stabilization Network), which functions as a power source of the circuit, and the AC-DC power converter.

In case of power-line frequency, the inductors are short, and the capacitors are open, while the inductors have high impedances and the capacitors have low impedances in case of the conducted EMI noise frequency.

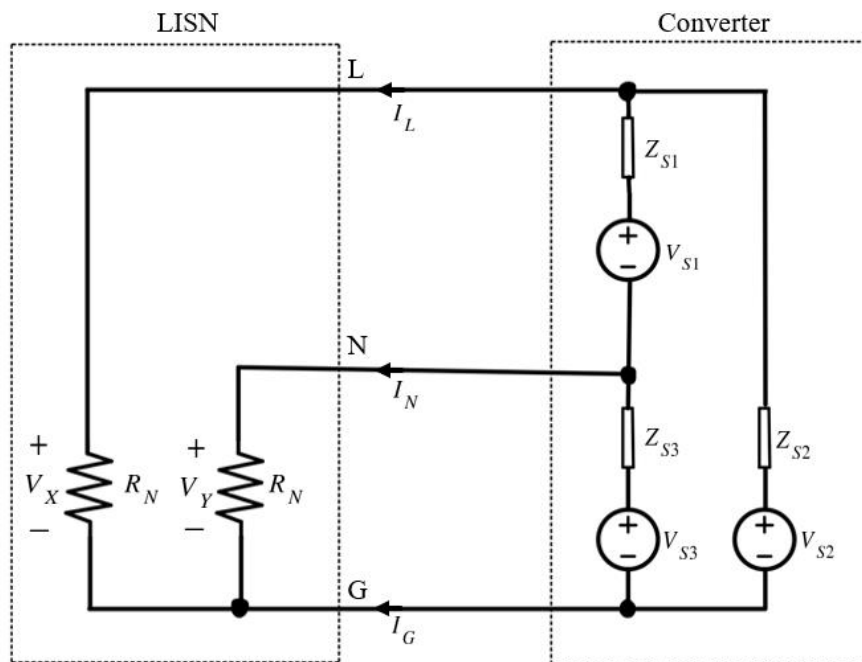


Fig. 3.8 Lumped circuit of EMI noise coupling

If we look deeply into the Fig. 3.7, the equation $V_X - V_Y$ refers to EMI noise in DM case and the equation $\frac{V_X + V_Y}{2}$ defines EMI noise in CM case. Also, V_{S1} and Z_{S1} belongs to the DM coupling, while V_{S2} , Z_{S2} , V_{S3} and Z_{S3} belongs to the CM coupling. Combining the above, it is expressed mathematically as the following:

$$V_{DM} = V_X - V_Y = R_N (I_L - I_N) \quad \dots \textcircled{a}$$

$$V_{CM} = \frac{V_X + V_Y}{2} = \frac{R_N (I_L + I_N)}{2} \quad \dots \textcircled{b}$$

$$(\because V_X = I_L R_N, V_Y = I_N R_N)$$

$$I_L = (V_{S1} - V_{DM}) / Z_{S1} + (V_{S2} - V_X) / Z_{S2} \quad \dots \textcircled{c}$$

$$I_N = - (V_{S1} - V_{DM}) / Z_{S1} + (V_{S3} - V_Y) / Z_{S3} \quad \dots \textcircled{d}$$

$$(\because KCL)$$

In the similar way as introduced in 3.1.2.1, we will assume that the topology of the AC-DC converter is balanced and has symmetry properties to reduce the complexity of modeling, i.e., $V_{S2} = V_{S3}$ and $Z_{S2} = Z_{S3}$. Therefore, the lumped circuit of EMI noise coupling can be simplified as shown in Fig. 3.9.

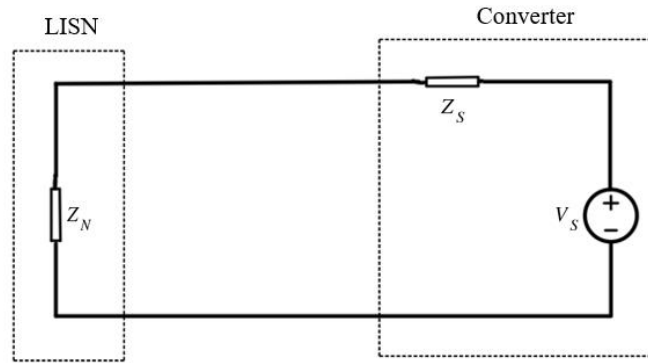


Fig. 3.9 Simplified lumped circuit of EMI noise coupling

Plus, the DM voltage and CM voltage can be reduced as

$$V_{DM} = \frac{2R_N V_{S1}}{Z_{S1} + 2R_N} \dots \textcircled{e} \text{ and } V_{CM} = \frac{R_N V_{S2}}{Z_{S2} + R_N} \dots \textcircled{f}$$

Lastly, the impedances Z_N and Z_S of each DM and CM case are shown in Table 3.1.

	DM	CM
Z_N	$2R_N$	$0.5R_N$
Z_S	Z_{S1}	$0.5Z_{S2}$

Table 3.1 Impedances in DM and CM case

3.2.1 DM noise source

When we analyze the EMI noise in the DM case, we are going to assign values of each parameter as the following. $R_N = 50\Omega$, $Z_{S1} = 50\Omega$, $V_{S1} = 12V$, and Z_{shunt} which consists of $R_N = 50\Omega$ and $C = 0.22\mu F$. By using these parameter values, we could easily

derive a value of V_{DM} by the equation $V_{DM} = \frac{2R_N V_{S1}}{Z_{S1} + 2R_N}$. Then, we can determine a DM model of EMI noise using a shunt-insertion method and applying the variables as shown in Fig.

3.10. Also, a precise way to check the value of V_{DM} is using a MATLAB code below.

```
clc;
clear;

R_n=50;
Z_s1=50;
V_s1=12;
V_dm=(2*R_n*V_s1)/(Z_s1+2*R_n);
C=0.22e-6;
L=1e-6;
```

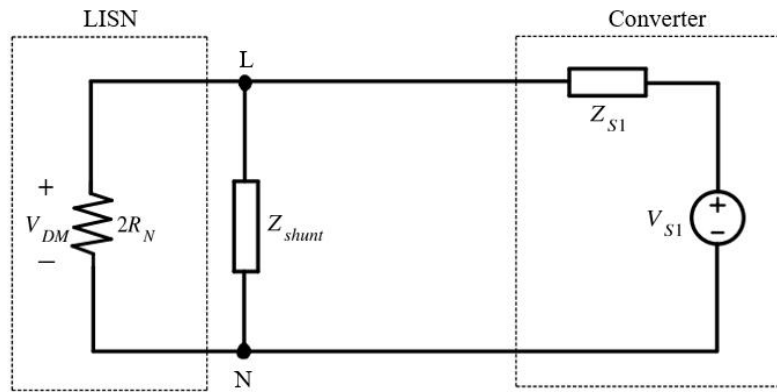


Fig. 3.10 DM model of EMI noise coupling

Since we have gone through the method to find the value of V_{DM} by the equation

$$V_{DM} = \frac{2R_N V_{S1}}{Z_{S1} + 2R_N}$$
, we must find another way to verify that this equation stands. The best way to establish it is to put the values of R_N , Z_{S1} , V_{S1} , L and C in the circuit elements and then run a simulation through Simulink, because we could simply define all the parameter values right away in Simulink if they exist in MATLAB workspace.

Before designing an actual circuit of DM model of EMI noise and running a simulation, we should first assume that the inductor L is negligible in the impedance Z_{S1} because the value is so small, and therefore we assigned the resistor value as Z_{S1} .

Next, we will find a relationship between V_{DM} and V_{S1} within a single simulation scope by using Mux operator, collecting data from the voltage sensors that are connected in parallel to $2R_N$ resistor and V_{S1} DC voltage source, using Goto operators for the simplicity of the circuit. The process above is well illustrated in Fig. 3.11.

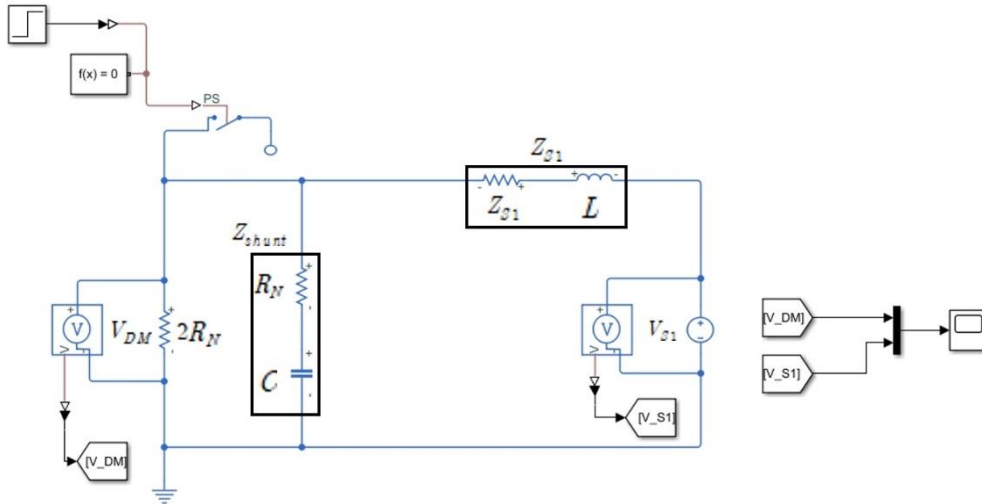


Fig. 3.11 DM modeling circuit using Simulink

3.2.2 CM noise source

The process is pretty much the same as the previous modeling in 3.2.1, but the configuration and values of each parameter are slightly different. We define the values $R_N = 50\Omega$, $Z_{s1} = 50\Omega$, $Z_{s2} = Z_{s3} = 500\Omega$, $Z_{series} = 1k\Omega$, $V_{s1} = V_{s2} = V_{s3} = 12V$ and $L = 1\mu H$. Then, we can determine a CM model of EMI noise using a series-insertion method and applying the variables as shown in Fig. 3.12. Next, we can find the values of I_L and I_N by the MATLAB code below.

```

clc;
clear;

R_n=50;
Z_s1=50;
Z_s2=500;
Z_s3=500;
Z_series=1000;
V_s1=12;
V_s2=12;
V_s3=12;
L=1e-6;

i_L=(R_n+Z_s2+V_s3+Z_s2*(R_n+Z_s3)+V_s1+(R_n+Z_s1+R_n+Z_s3+Z_s1+Z_s3)+V_s2)/(Z_s1+Z_s2+Z_s3+R_n^2*(Z_s1+Z_s2+Z_s3)+R_n*(Z_s1+Z_s2+Z_s1+Z_s3+2*Z_s2+Z_s3));
i_N=(R_n+Z_s3+V_s2+Z_s3*(R_n+Z_s2)+V_s1+(R_n+Z_s1+R_n+Z_s2+Z_s1+Z_s2)+V_s3)/(Z_s1+Z_s2+Z_s3+R_n^2*(Z_s1+Z_s2+Z_s3)+R_n*(Z_s1+Z_s2+Z_s1+Z_s3+2*Z_s2+Z_s3));

```

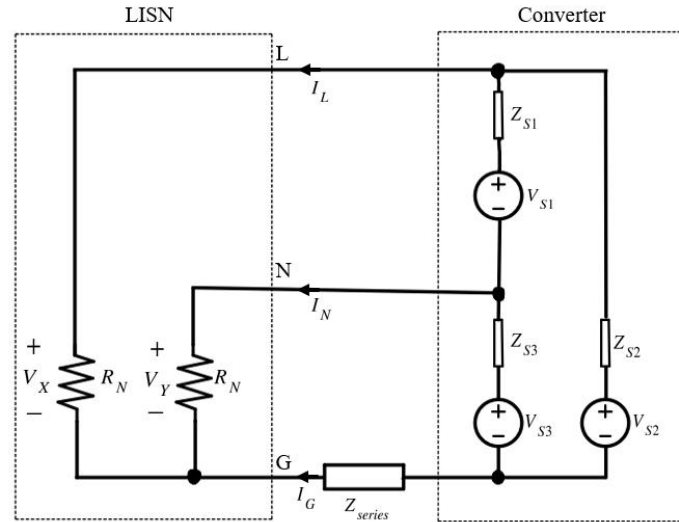


Fig. 3.12 CM model of EMI noise coupling

Since we have gone through the mathematical way to find the value of I_L and I_N by

the equation
$$I_L = \frac{R_N Z_{S2} V_{S3} + Z_{S2} (R_N + Z_{S3}) V_{S1} + (R_N Z_{S1} + R_N Z_{S3} + Z_{S1} Z_{S3}) V_{S2}}{Z_{S1} Z_{S2} Z_{S3} + R_N^2 (Z_{S1} + Z_{S2} + Z_{S3}) + R_N (Z_{S1} Z_{S2} + Z_{S1} Z_{S3} + 2 Z_{S2} Z_{S3})}$$

and
$$I_N = \frac{R_N Z_{S3} V_{S2} - Z_{S3} (R_N + Z_{S2}) V_{S1} + (R_N Z_{S1} + R_N Z_{S2} + Z_{S1} Z_{S2}) V_{S3}}{Z_{S1} Z_{S2} Z_{S3} + R_N^2 (Z_{S1} + Z_{S2} + Z_{S3}) + R_N (Z_{S1} Z_{S2} + Z_{S1} Z_{S3} + 2 Z_{S2} Z_{S3})}$$
, we

should find another way to verify that this equation stands.

We will find the values of V_x , V_v , I_L and I_N by running a simulation through Simulink and then compare them with the values that are deduced with the mathematical approach previously. Since the circuit is much more complex than the DM modeling circuit as shown in Fig. 3.12, we expect that there would be some errors, which we will figure out in 4.2.2.

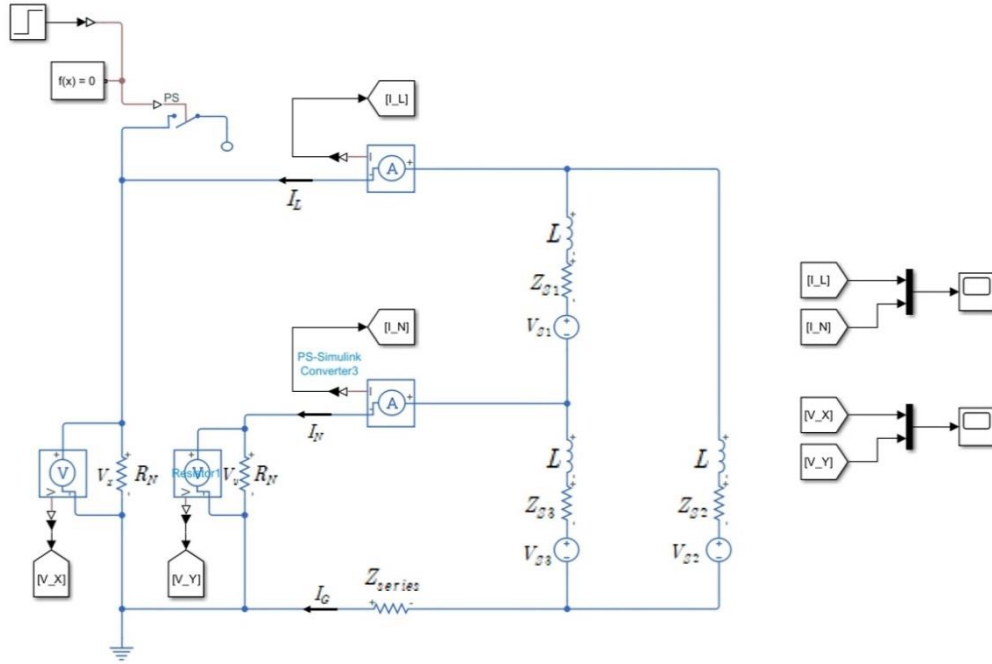


Fig. 3.13 CM modeling circuit using Simulink

4. Comparative verification of modeling-based analysis and simulation results

Based on the theory so far, both DC cable modeling and power converter modeling design have been carried out. We would like to confirm and analyze the results of these designs respectively.

4.1 Based on noise source modeling applied to DC line

4.1.1 Verification of mathematical approach

As we made the DC equivalent circuit of the 3-conductor cable as in 3.1.2.2 Fig. 3.6, we would like to verify the matrices and equations ③~⑥ in 3.1.2.2. Therefore, we assign the appropriate values of each variable, form the admittance matrix consisting of y-parameters, and then transform it to scattering matrix using the equation ⑥ in 3.1.1.2, as shown in the MATLAB code below.

```
clc;
clear;

n=3;
R=50;
R_sh=50;
R_g=50*10^6;
V1=12;
V2=12;
V3=12;
V4=11.5;
V5=11.5;
V6=11.5;

Z_0=50;

y_s=1/R_g+1/(R+(1/((n-1)/R+1/R_sh)));
y_m=-1/(R+(1/((n-1)/R+1/R_sh)));
y_m1=(1/(n-1+R/R_sh))*(1/(R+(1/((n-1)/R+1/R_sh))));

Y_s=[y_s y_m1 y_m1;
      y_m1 y_s y_m1;
      y_m1 y_m1 y_s];

Y_m=[y_m -y_m1 -y_m1;
      -y_m1 y_m -y_m1;
      -y_m1 -y_m1 y_m];

Y_dc=[Y_s Y_m;
      Y_m Y_s];

S=j*inv(ones(6)+Z_0.*Y_dc)*(ones(6)-Z_0.*Y_dc);
```

```

>> Y_dc

Y_dc =

    0.0150    0.0050    0.0050   -0.0150   -0.0050   -0.0050
    0.0050    0.0150    0.0050   -0.0050   -0.0150   -0.0050
    0.0050    0.0050    0.0150   -0.0050   -0.0050   -0.0150
   -0.0150   -0.0050   -0.0050    0.0150    0.0050    0.0050
   -0.0050   -0.0150   -0.0050    0.0050    0.0150    0.0050
   -0.0050   -0.0050   -0.0150    0.0050    0.0050    0.0150

>> S

S =

  -0.6667    0.3333    0.3333    0.3333    0.3333    0.3333
    0.3333   -0.6667    0.3333    0.3333    0.3333    0.3333
    0.3333    0.3333   -0.6667    0.3333    0.3333    0.3333
    0.3333    0.3333    0.3333   -0.6667    0.3333    0.3333
    0.3333    0.3333    0.3333    0.3333   -0.6667    0.3333
    0.3333    0.3333    0.3333    0.3333    0.3333   -0.6667

```

When we take a look at the result from the MATLAB code above, we can see that the values of y-parameters deduced by the ports in the same lines are different from the values of y-parameters deduced by the ports in the different lines in Y_{dc} . Also, the values of y-parameters of the matrix ⑥ and ⑦ in 3.1.2.2 are almost the same except for the opposite sign.

Lastly, we can see that the scattering matrix also follows a similar form of the matrix ⑧ in 3.1.1.2, which implies that it satisfied the equation ⑨ in 3.1.1.2 and the DC equivalent circuit of the 3-conductor cable is valid.

4.1.2 Analyzing the characteristics of actual cable model

As we go through the experiment within the frequency range of 150kHz~30MHz, we setup the simulation frequency range as in Fig. 4.1 below.

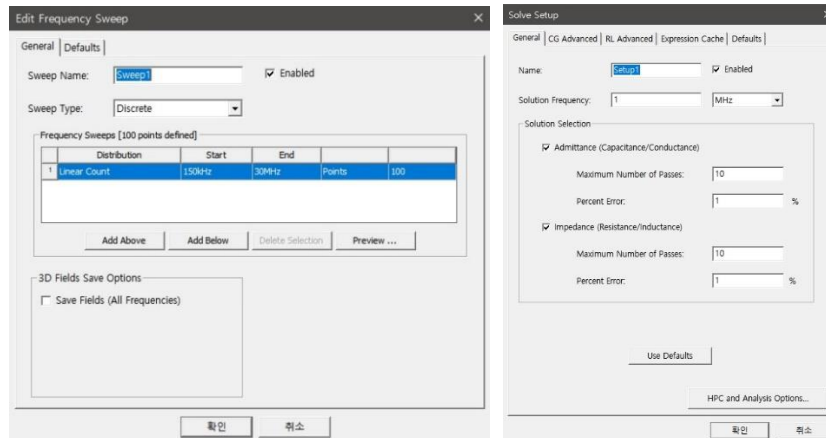


Fig. 4.1 Simulation setup

Looking at the C Matrix plot in Fig. 4.2, we can find out that the capacitance is reduced to a value of $112.61873\mu F$. When modeling DC equivalent circuit as in 3.1.2.2, it was confirmed that the impedance between the lines was made with only a resistor, and we can judge that the capacitance is negligible as the value decreases dramatically.

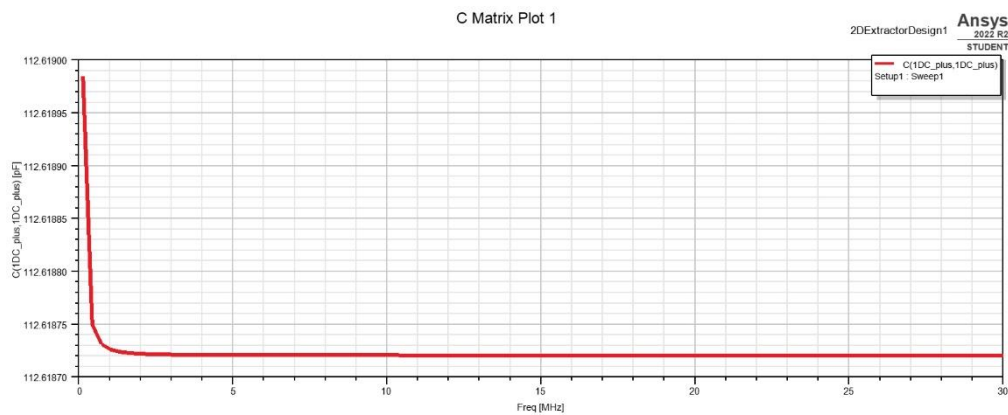


Fig. 4.2 C Matrix plot of the cable model

When we look at the Characteristic Impedance plot in Fig. 4.3, it shows the characteristic impedance of both the DC plus line and the PP line, 135Ω and 87.5Ω respectively. By the equation $R = \frac{\rho S}{L}$, we can see that the impedance is proportional to the cross-section area S

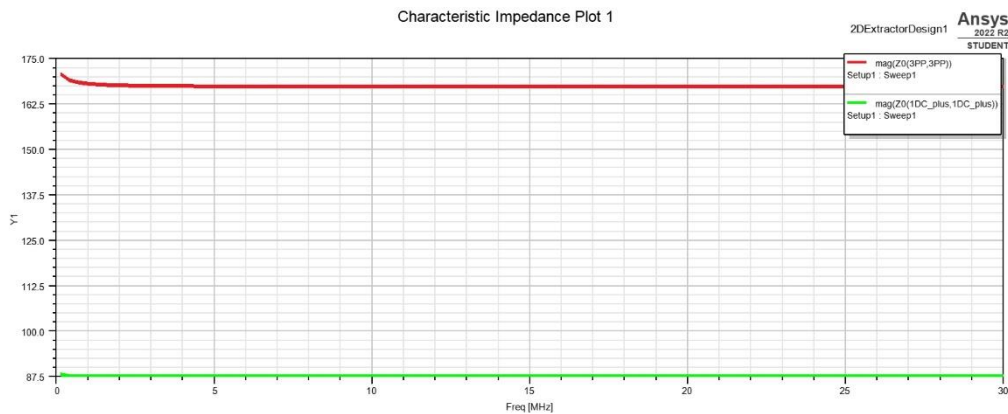


Fig. 4.3 Characteristic Impedance plot of the cable model

Finally, looking at the R Matrix plot in Fig.4.4, It can be seen that the R value decreases in proportion to the distance between the lines. It is revealed that this is because the farther the distance between the lines, the smaller the mutual interference between them.

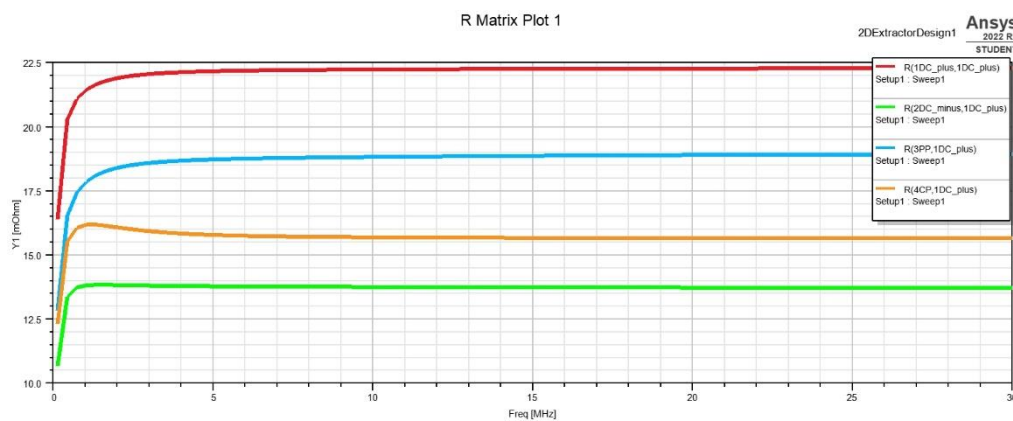


Fig. 4.4 R Matrix plot of the cable model

4.2 Based on noise source modeling according to the topology of the power converter

4.2.1 DM noise source

When we check the value of V_{DM} by mathematical analysis using the MATLAB code, it is shown as the following result.

```
>> V_dm
```

```
V_dm =
```

```
8
```

Looking at the simulation result from Fig. 4.5, we can see that the value of V_{S1} (blue) is $12V$ and the value of V_{DM} (yellow) is $8V$. Substituting the values in the equation $V_{DM} = \frac{2R_N V_{S1}}{Z_{S1} + 2R_N}$, it is derived as $\frac{2 \times 50}{50 + 2 \times 50} \times 12 = 8$, which implies that the DM modeling of EMI noise is valid.

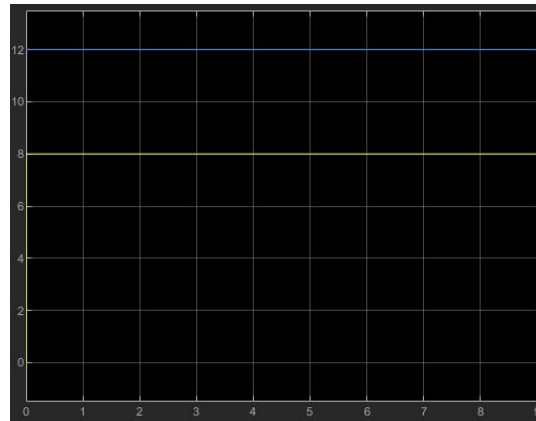


Fig. 4.5 Simulation result of voltage in DM modeling circuit

4.2.2 CM noise source

When we check the values of I_L and I_N by mathematical analysis using the MATLAB code, it is shown as the following result.

```
>> i_L, i_N
```

```
i_L =
```

```
0.0992
```

```
i_N =
```

```
-0.0556
```

Looking at the simulation result from Fig. 4.6 and using a cursor function as shown in Fig. 4.7,

we can see that the value of I_L (yellow) is $0.0821A$ and the value of I_N (blue) is $-0.0727A$.

Comparing the results between MATLAB and Simulink, the error of I_L is

$$\frac{|0.0992 - 0.0821|}{0.0992} \times 100(\%) = 17.24\% \quad \text{and the error of } I_N \text{ is } \left| \frac{-0.0556 - (-0.0727)}{-0.0556} \right| \times 100(\%) = 30.76\%.$$

We can see that the errors are a bit high, but still, it implies that the CM modeling of EMI noise is valid.

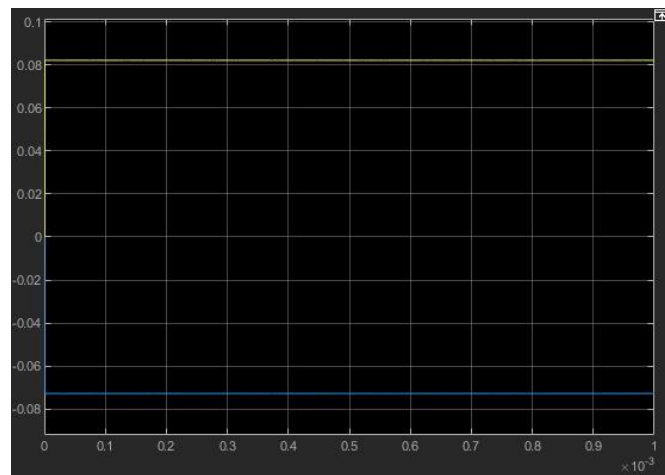


Fig. 4.6 Simulation result of current in CM modeling circuit

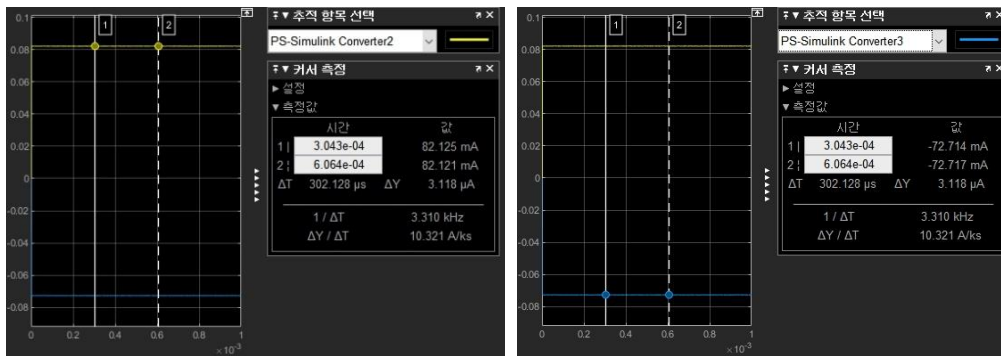


Fig. 4.7 Checking current with cursor

We also have to go through a validation of the voltage values V_x and V_v . Looking at the simulation result from Fig. 4.8 and using a cursor function as shown in Fig. 4.9, we can see that the value of V_x (yellow) is $4.106 V$ and the value of V_v (blue) is $-3.636 V$. As the value of I_N is negative, it is reasonable that the value of V_v is also negative.

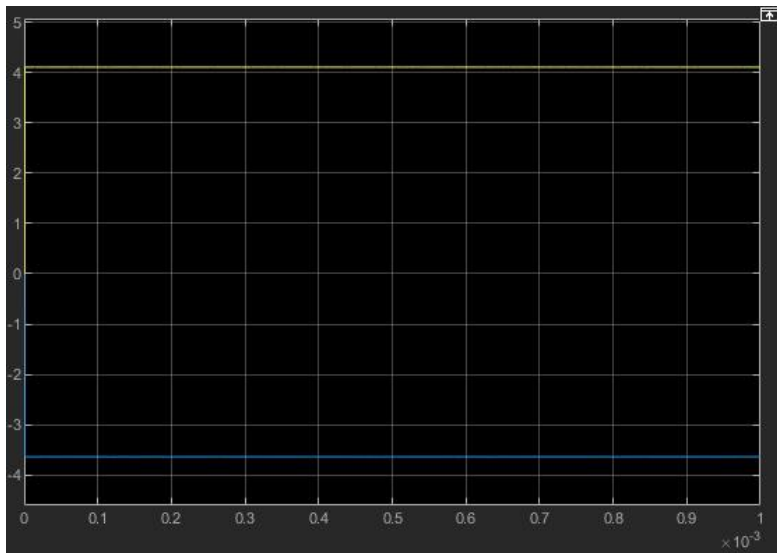


Fig. 4.8 Simulation result of voltage in CM modeling circuit

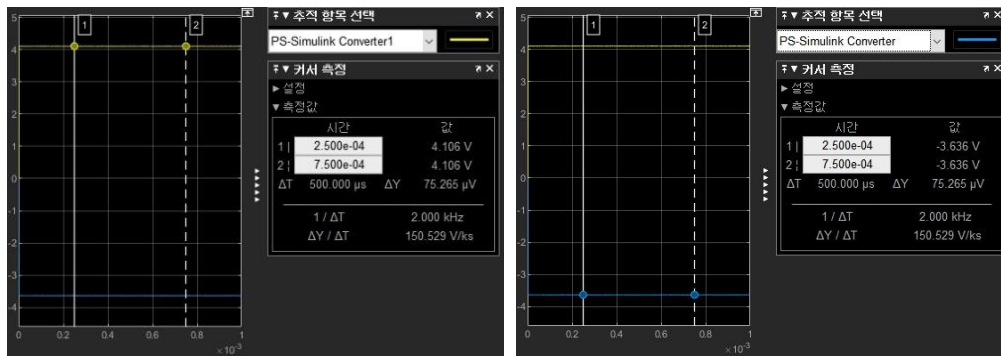


Fig. 4.9 Checking voltage with cursor

When we substitute the values of V_x and V_y in the equation

$$V_{s2} = V_x + \frac{V_x + V_y}{R_N} Z_{series} + \left[\frac{V_x}{R_N} - \frac{V_{s1} - (V_x - V_y)}{Z_{s1}} \right] Z_{s2} \text{ using MATLAB as below,}$$

```
clc;
clear;
```

```
R_n=50;
Z_s1=50;
Z_s2=500;
Z_s3=500;
Z_series=1000;
V_s1=12;
```

```
>> V_s2
```

```
V_x=4.106;
V_y=-3.636;
```

```
V_s2 =
```

```
V_s2=V_x+((V_x+V_y)/R_n)+Z_series+(V_x/R_n-(V_s1-(V_x-V_y))/Z_s1)+Z_s2; => 11.9860
```

the result shows that V_{s2} and V_{s3} are $12V$, since we assumed that $V_{s2} = V_{s3}$ in the beginning of the mathematical analysis, and it implies that the CM modeling of EMI noise is valid because they match with the values that we designated.

5. Review and discussion

Honestly, according to the original plan, in cases of the noise source modeling applied to the DC line and the noise source modeling according to the topology of the power converter respectively, I was going to construct circuits and equations through mathematical methods in the first step, conduct simulation experiments through MATLAB, Simulink, and Ansys Electronics programs in the second step, and make an experiment with real cables and real power converters in the last step. After that, I was planning to conduct error analysis by comparing and contrasting the results derived from theory, simulation results, and actual measurement results. However, I had not learned the essential major subjects I had to learn before proceeding with this research, and because there was no experimental equipment for conducting actual experiments and no knowledge to handle the equipment, the research was conducted only through mathematical approaches and simulation experiments unfortunately.

Although the research didn't go well as I intended, I have no regrets in choosing this research topic in the sense that I was able to get an overall idea of the electric vehicle field I hope to work in the future and understand to a certain extent about electric vehicle fast charging cables and think of ways to improve problems. What I have clearly realized through this study is that in the multi-conductor cable modeling, the voltage and current applied to each port on the same line are little bit different due to EMI noise, so noise analysis is carried out using a scattering matrix in the high frequency region. Also, in the power converter noise modeling, I've understood that the reason for making a dc equivalent circuit is to simplify mathematical calculations and modeling.

The reason for conducting this research in the first place is to improve the problem of electric vehicle fast charger and to develop more efficiently. Therefore, I thought that it would be much better if modeling was carried out considering techniques to reduce EMI noise generated by DC/DC converters, such as spread spectrum techniques, chaotic soft-switching techniques, active filtering, and PCB layout modification.

6. Conclusion

In this study, we identified the overall process of modeling the noise source applied to the DC line and modeling the noise source according to the topology of the power converter respectively, and then conducted simulation experiments for both modeling.

First, in the case of modeling the noise source applied to the DC line, we figured out how the admittance matrix and scattering matrix are formed in the overall case, that is, in the case of multi-conductor cable, and then how the admittance matrix and scattering matrix are formed in the case of 3-conductor cable. It was figured out in detail through the MATLAB program by forming a specific variable setting and configuration and designing an equivalent circuit of the cable. In the CCS Combo Type 1 cable model, which is a cable that we use in real life, what kind of simulation results are produced according to the characteristics of each line itself or the relationship between the lines that can be seen through the cross-section of the model, were confirmed through the Ansys Electronics program.

Next, in the case of the noise source modeling according to the topology of the power converter, since the circuit of the actual power converter is too complicated and it is almost impossible to model it right away, simplification was carried out by making a lumped circuit of EMI noise coupling. After that, the model was constructed by dividing the cases into the Differential mode(DM) and the Common mode(CM) after organizing and defining each element and parameter value of the circuit through various equations, using MATLAB and Simulink program.

Lastly, we compared and contrasted the result values or simulation results that were deduced by the method of directly substituting the variable values and specifying the parameters with the results obtained by mathematical approach to prove the validity of the models for both modeling cases. Later, we analyzed the simulation results of the CCS Combo Type 1 cable using the information that can be grasped through the cross section of the cable model.

Reference

- [1] Paul, Clayton R. 2006. Introduction to electromagnetic compatibility.
- [2] "Combined Charging System", Wikipedia, last modified July 27, 2022, accessed July 31, 2022, https://en.wikipedia.org/wiki/Combined_Charging_System
- [3] "DC 고속 충전기 포인트용 CCS 유형 1 플러그 J1772 콤보 1 커넥터 SAE J1772-2009", MiDA, last modified April 17, 2021, accessed July 31, 2022, <https://www.midaevse.com/ko/news/ccs-type-1-plug-j1772-combo-1-connector-sae-j1772-2009-for-dc-fast-charger-point/>
- [4] 정일순.(2021).전기차 충전기 전력변환장치 개요.KIPE MAGAZINE,26(3),64-67.
- [5] "Electric power conversion", Wikipedia, last modified December 6, 2021, accessed July 31, 2022, https://en.wikipedia.org/wiki/Electric_power_conversion#DC_to_DC
- [6] "스위치 모드 파워 서플라이", 위키백과, last modified February 6, 2022, accessed July 31, 2022, https://ko.wikipedia.org/wiki/%EC%8A%A4%EC%9C%84%EC%B9%98_%EB%AA%A8%EB%93%9C_%ED%8C%8C%EC%9B%8C_%EC%84%9C%ED%94%8C%EB%9D%BC%EC%9D%B4
- [7] I. Stevanović, B. Wunsch, G. L. Madonna and S. Skibin, "High-Frequency Behavioral Multiconductor Cable Modeling for EMI Simulations in Power Electronics," in IEEE Transactions on Industrial Informatics, vol. 10, no. 2, pp. 1392-1400, May 2014, doi: 10.1109/TII.2014.2307198.
- [8] J. Meng, W. Ma, Q. Pan, Z. Zhao and L. Zhang, "Noise Source Lumped Circuit Modeling and Identification for Power Converters," in IEEE Transactions on Industrial Electronics, vol. 53, no. 6, pp. 1853-1861, Dec. 2006, doi: 10.1109/TIE.2006.885129.

국 문 요 약

고 전력 충전 시스템에서의 전자파 간섭 해석 및 측정

본 연구는 전기차 관련 기술이 발전함에 따라 급속 충전 시스템에 대한 관심이 많아지고 운전자의 편의성을 개선하기 위해 고전력을 이용하는 고속 충전 시스템의 필요성이 증대됨에 따라 DC line에 인가되는 noise source 모델링과 전력 변환기의 topology에 따른 noise source 모델링을 진행한 후, 이러한 모델링 기반의 해석 및 시뮬레이션 결과를 비교 검증하는 것을 목표로 한다. 케이블 노이즈 모델링의 경우, 먼저 케이블이 3-conductor cable이라는 것을 전제로 DC 등가회로를 형성하였다. 이때 회로는 고주파 영역에서 동작을 하기 때문에 같은 선상에서 두 포트에 인가되는 전압과 전류의 값이 다르고 선 사이에 EMI 노이즈가 발생하기 때문에 admittance matrix와 scattering matrix를 사용하여 모델링을 진행한다. 각 소자 및 파라미터에 값을 대입하고 시뮬레이션 실험을 해봄으로써 모델링의 타당성을 입증하였다. 전력 변환기 노이즈 모델링의 경우, EMI 노이즈 커플링의 집중 회로가 신호의 방향에 의해 전도 노이즈 모드가 바뀌면서 구성이 달라지기 때문에 DM 모델과 CM 모델로 나누어 진행하였다. DM 노이즈 모델링에서는 shunt-insertion 방법을 사용하여 회로를 구성하고, CM 노이즈 모델링에서는 series-insertion 방법을 사용하여 회로를 구성하고, 각 소자 및 파라미터에 값을 대입하고 시뮬레이션 실험을 해봄으로써 두 모델링의 타당성을 모두 입증하였다.

핵심되는 말 : EMI, multi-conductor cable, admittance matrix, scattering matrix, DM, CM